Hybrid polymer composites for medical applications as artificial bone

Katarzyna Bulanda[1),*)] (ORCID ID: 0000-0002-5330-5719), **Damian Filip**[2)] (0000-0002-5291-3501), **Małgorzata Oleksy**[3)]

DOI: https://doi.org/10.14314/polimery.2025.7.6

Abstract: The effect of filler type and amount ($CaCO_3$, silica, hydroxyapatite, perlite) on the Rockwell hardness, compressive strength, and Young's modulus of polymer composites intended for medical applications as artificial bones was investigated. The bone models were made in the form of cylinders with an EP-based coating containing selected fillers imitating solid bone tissue. The cylinder core (porous, soft tissue) was polyurethane foam (PUR). Samples for mechanical properties were obtained using the vacuum casting (VC) method. The composite containing 35 wt% $CaCO_3$, 4 wt% hydroxyapatite, 4 wt% perlite, and 4 wt% silica (P47) had properties most like natural bone. The developed anatomical models can be used for practical exercises and surgical planning in orthopedics and veterinary medicine.

Keywords: artificial bone, polymer composites, fillers, mechanical properties.

Hybrydowe kompozyty polimerowe do zastosowań medycznych jako sztuczne kości

Streszczenie: Zbadano wpływ rodzaju oraz ilości napełniacza ($CaCO_3$, krzemionka, hydroksyapatyt, perlit) na twardość Rockwella, wytrzymałość na ściskanie i moduł Younga kompozytów polimerowych przeznaczonych do zastosowań medycznych jako sztuczne kości. Modele kości wykonano w kształcie walców z otoczką na osnowie EP z dodatkiem wytypowanych napełniaczy, imitującą tkankę litą kości. Rdzeń walca (tkankę miękką porowatą) stanowiła pianka poliuretanowa (PUR). Próbki do badań mechanicznych otrzymano metodą odlewania próżniowego (VC). Kompozyt zawierający 35% mas. $CaCO_3$, 4% mas. hydroksyapatytu, 4% mas. perlitu oraz 4% mas. krzemionki (P47) miał właściwości najbardziej zbliżone do naturalnej kości. Opracowane modele anatomiczne mogą służyć do ćwiczeń praktycznych i planowania zabiegów operacyjnych w ortopedii i weterynarii.

Słowa kluczowe: sztuczna kość, kompozyty polimerowe, napełniacze, właściwości mechaniczne

The use of polymeric materials in medicine is extensive and rapidly expanding. Polymers, both natural and synthetic, are used in many fields of medicine due to their properties, such as lightness, flexibility, biocompatibility, ease of forming, and the ability to control their degradation [1, 2].

For a polymeric material to replace natural bone, it must possess the following characteristics: adequate mechanical strength (especially compressive strength), biocompatibility (not triggering an immunological reaction), sometimes bioresorbability (the material degrades within the body), the ability to interact with bone cells (osseointegration), and a structure enabling bone tissue growth (porosity) [3, 4].

In recent years, we have observed a dynamic development in the use of rapid prototyping technologies using polymeric materials to create anatomical structures. Models made from basic, unmodified polymeric materials are most often used as conceptual prototypes, as these materials do not provide adequate functionality, the necessary mechanical strength, or functional properties of the components. For this reason, it is necessary to intensify research on the modification of previously used polymer materials. Significant progress has been made in the development of polymer composites, which, thanks to their improved functional properties, can be successfully used to produce functional models using additive manufacturing techniques, including vacuum casting (VC). Vacuum casting is one of the oldest techniques, allowing to produce high-quality components with high precision of detail reproduction. The process is characterized by short processing times and low production costs, allowing for rapid and economical reproduction of proto-

[1)] Department of Polymer Composites, Faculty of Chemistry, Rzeszów University of Technology, al. Powstańców Warszawy 6, 35-959 Rzeszów, Poland.

[2)] Institute of Medicine, College for Medical Sciences of University of Rzeszów, al. Rejtana 16c, 35-959 Rzeszów, Poland.

[3)] Students Medical College of the University of Rzeszów, University of Rzeszów, al. Kopisto 2A, 35-959 Rzeszów, Poland.

[*)] Author for correspondence: k.bulanda@prz.edu.pl

types [5]. This technique was used to duplicate a hip bone prototype. Despite its advantages, VC process also has disadvantages. Casting is associated with the presence of casting shrinkage, the formation of misruns, and leaks. These phenomena are related to incorrect pressure regulation; therefore, continuous monitoring is necessary. A major disadvantage is the short lifespan of silicone molds [6]. The advantages of VC technology in creating artificial bones include:

– high accuracy of reproduction – the ability to obtain highly detailed anatomical structures (e.g., trabeculae);

– porosity control – crucial for imitating natural bone, enabling tissue integration;

– the ability to use various polymer materials – e.g., polyurethanes, epoxy resins, silicones;

– cost-effectiveness – a cheaper and faster alternative to 3D printing for mass production;

– compatibility with medical data – the ability to create individual models based on CT/MRI scans.

The resulting artificial bone models obtained using the VC method can be used as:

– models for training in orthopedic and dental surgery,

– phantoms for medical imaging (X-ray, CT, MRI),

– implants and scaffolds in tissue engineering (after material modifications),

– demonstration models for surgical planning and patient education.

Summarizing literature reports and our own experience, vacuum casting technology is an effective method for obtaining artificial bone with a high degree of anatomical reproduction and a controlled porous structure. It is primarily used in educational and diagnostic modeling, as well as prototyping implants and tissue engineering structures.

The work presented in this article is a continuation of the authors' previous research [1]. Therefore, the aim of the study was to obtain hybrid polymer composites using the vacuum casting (VC) method, intended for use as artificial bone models. The effect of the type and amount of filler ($CaCO_3$, silica, hydroxyapatite, perlite) on the Rockwell hardness, compressive strength, and Young's modulus of the obtained composites was investigated. The bone models were made in the form of cylinders with an EP-based coating containing selected fillers (hard bone tissue) and a PUR foam core (porous, soft tissue).

EXPERIMENTAL PART

Materials

In this research, following materials was used: calcium carbonate ($CaCO_3$) (Warchem Ltd. Poland), dabco-1,4-diazabicyclo[2.2.2]octane (Merck KGaA, Germany), epoxy resin Epidian 624 (Sarzyna Chemical Ltd., Poland), ABS filament (Spectrum Filaments, Poland), ethylene glycol (Chemer Pol-Aura, Poland), hardener Z1 (Sarzyna Chemical Ltd., Poland), silica Aerosil MOX 120 (OQEMA Ltd., Poland), MDI-4,4'-diisocyanate-diphenylmethane (Chem Distribution, The Netherlands), perlite (ZGM Zębiec SA, Poland), hydroxyapatite, Rokopol M1170 (PCC Rokita S.A./Polyol Complex, Poland), silicone ZA 22 MOULD (Zhermack SpA – Via Bovazecchino, Italy).

Sample preparation

The preparation of the artificial bone prototype was conducted in three stages, according to the procedure published elsewhere [1]. In the first stage, models were prepared from ABS filaments, which were used to produce a silicone mold in a similar manner as described in [1]. Next, the silicone mold was divided into two parts along the separation plane so that the model could be easily removed after VC casting. Subsequently, resin mixtures with selected fillers were prepared using a high-speed homogenizer (Dispermat, type D-51580, with a turbine mixer, Getzmann GmbH, Germany) for approximately 30 min at various speeds (500–2500 rpm). Then, 12 wt% of hardener was added to each mixture. The prepared mixture was filled into silicone molds to create an external element in the form of a hollow cylinder of bone prototypes. In the third stage, a specially prepared polyurethane foam composition was introduced into the resulting cylindrical artificial bone fragments.

The compositions of EP and PUR-based composites are summarized in Tables 1 and 2, respectively. Figure 1 shows the bone prototypes.

Methods

Rockwell hardness was measured in accordance with the PN-EN ISO 6508 standard using a Zwick/Roell hardness tester (Zwick GmbH & Co., Ulm, Germany) at ambient temperature under a load of 132 N (samples without

T a b l e 1. Composition of EP-based composites

Sample	Filler content, wt%			
	Calcium carbonate	Hydroxyapatite	Perlite	Silica
P0	–	–	–	–
P42	30	4	4	4
P47	35	4	4	4
P52	40	4	4	4

T a b l e 2. Composition of composites based on PUR foam

Material	Content, wt%
Rokopol G441 - Polyol	29.9
MDI - 4,4'-diphenylmethane diisocyanate	64.4
Ethylene glycol	3.3
Water	1.7
DABCO - 1,4-diazabicyclo[2.2.2]octane	0.8
Silicone	0.4

Fig. 1. Bone prototypes

Fig. 2. Samples for compression testing

filler) and 385 N (samples with filler). Ten determinations were made for each series.

Compressive properties were determined in accordance with the PN-EN ISO 604 standard using an Instron 5967 tensile testing machine (Instron, Grove City, Pennsylvania, USA) and the Aramis optical system.

Young's modulus was measured in accordance with the PN-EN ISO 527 standard on an Instron 5967 tensile testing machine (Instron, Grove City, Pennsylvania, USA) at a tensile rate of 5 mm/min (to 1% tensile strain). The sample surface was coated with a layer of white paint. After the paint dried, randomly distributed black dots were applied, creating a contrasting pattern necessary for the proper operation of the Aramis system (Fig. 2).

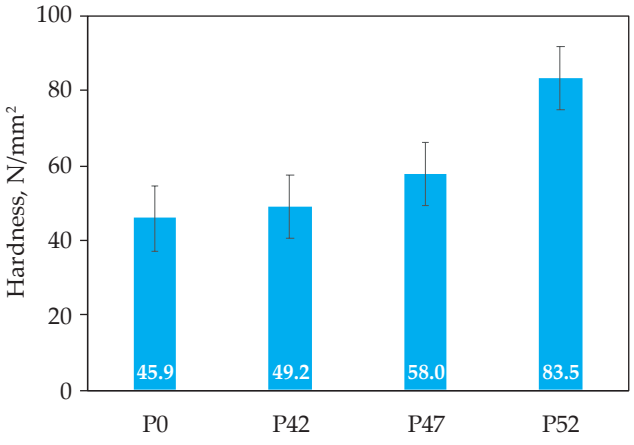

Fig. 3. Hardness of the samples

Microscopic images were taken using an SX45-TR stereomicroscope (Vision Engineering, Woking Surrey, UK) at two magnifications (2× and 5×), and the PUR pore sizes were measured.

RESULTS AND DISCUSSION

Hardness

Figure 3 shows Rockwell hardness of the composites. The hardness increased with increasing filler content up to approximately 82% in the case of P62 composite. The results are consistent with previous reports [7–11].

Compression properties

Figures 4–11 present the visualization of the displacement resulting from the action of the maximum load on the sample positioned in the apparatus vertically and horizontally in three axes: X, Y and Z. The largest displacement of the sample is visualized in red, and the smallest in blue color.

Figure 4 shows the displacement for the unfilled sample. The force applied to the sample reached a maximum value of 21.34 kN for the vertical sample. The largest displacement of the sample positioned vertically in the apparatus, in the X, Y, and Z axes, reached 0.333 mm, -0.499 mm, and 1.032 mm, respectively. The largest displacement was observed in the Z axis, at the center of the sample. The smallest deformation occurred on the X axis.

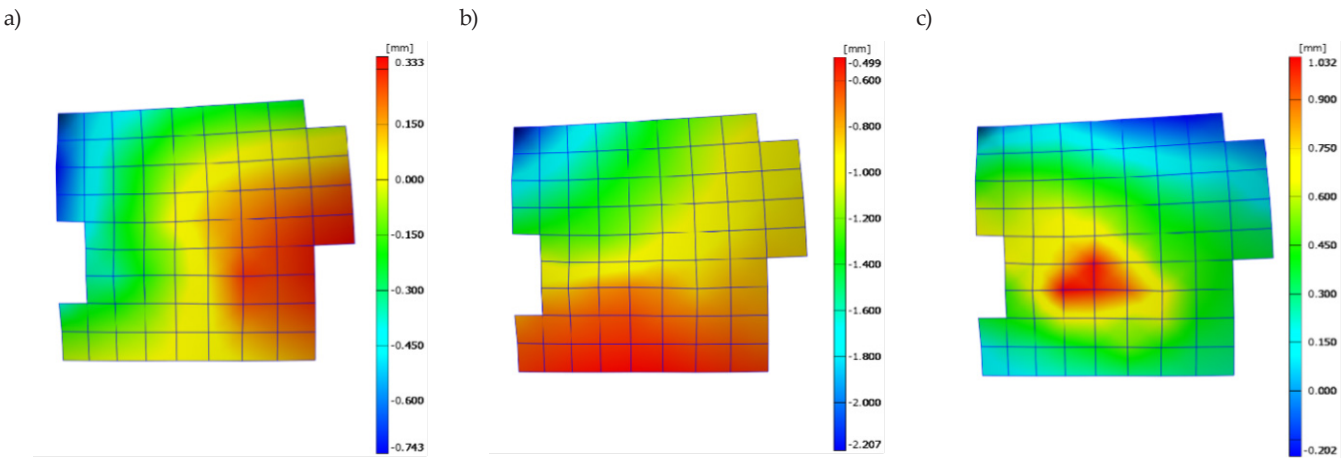

Fig. 4. Displacement distribution of an unfilled sample placed vertically: a) X axis, b) Y axis, c) Z axis

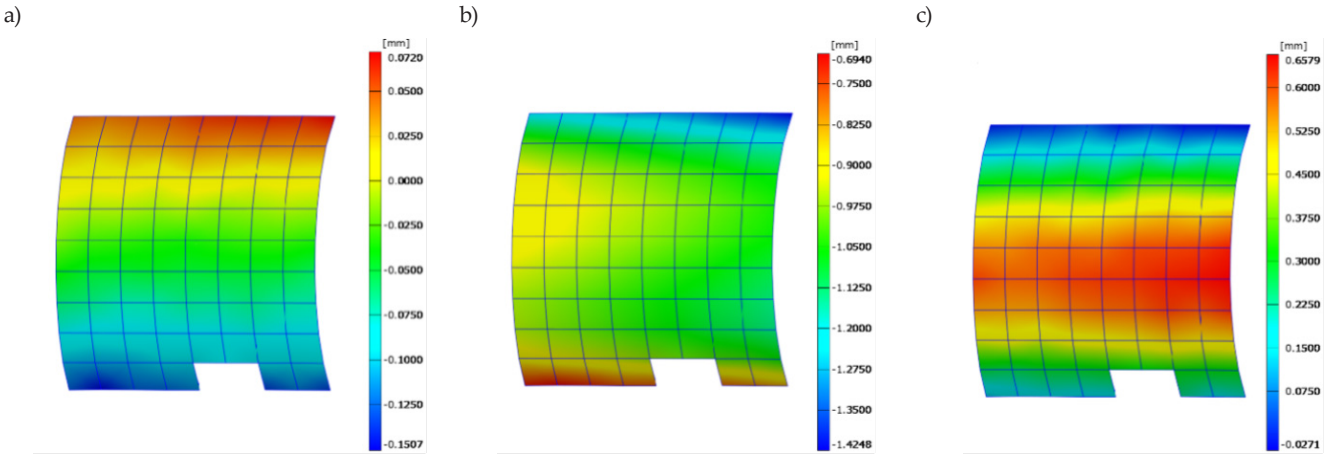

Fig. 5. Displacement distribution of the unfilled sample placed horizontally: a) X axis, b) Y axis, c) Z axis

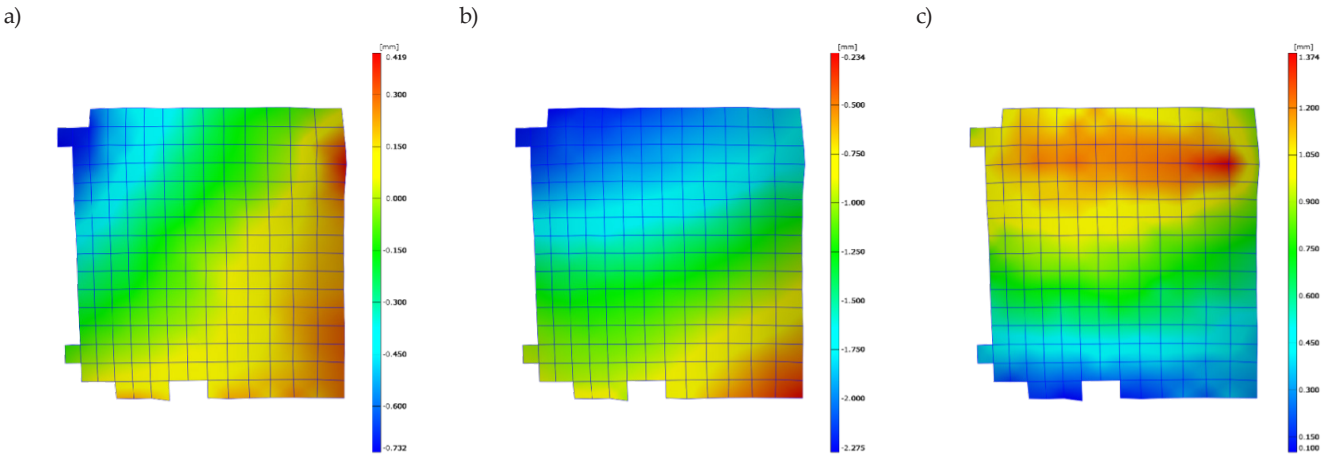

Fig. 6. Displacement distribution of P42 sample placed vertically: a) X axis, b) Y axis, c) Z axis

Figure 5 shows maps of the displacement distribution in three axes for a sample placed horizontally in the apparatus. The displacement resulting from the application of a maximum force of 1.70 kN reaches 0.072 mm on the X axis, -0.694 mm in the Y axis, and 0.658 mm in the Z axis. Displacement in the Z axis showed that uniform displacement occurred in the central part of the sample. The smallest defects were observed for the horizontal sample in the X axis (Fig. 5), where the maximum displacement occurred at the point of force application.

Figure 6 shows the displacement of a sample containing 30 wt.% calcium carbonate and 4% silica, hydroxyapatite, and pearlite (total filling 42 wt.%). A force was applied to the sample, the maximum value of which in the vertical position reached 24.20 kN. The largest displacement of the sample positioned vertically in the apparatus, in the X, Y,

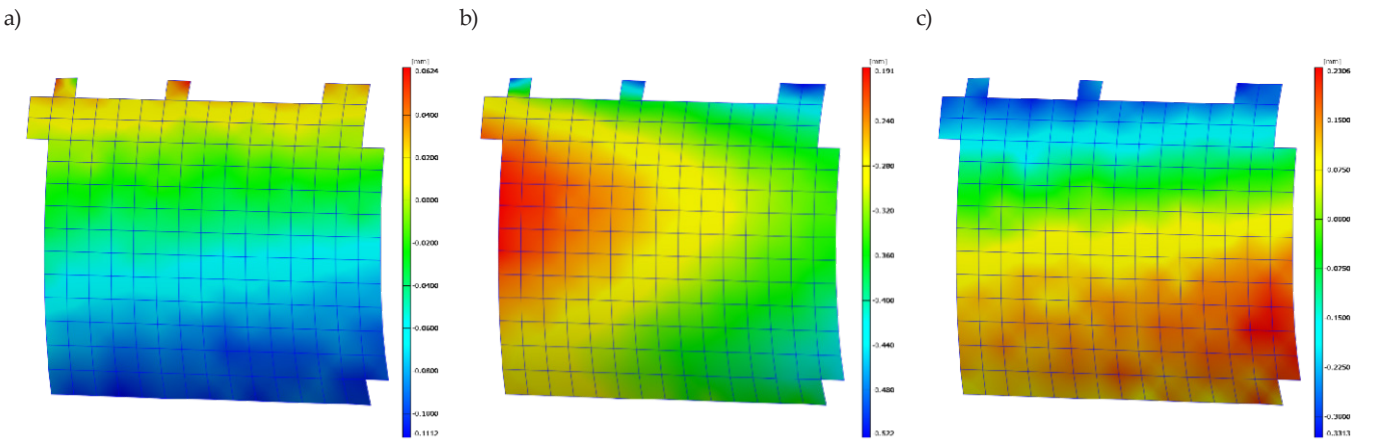

Fig. 7. Displacement distribution of P42 sample placed horizontally: a) X axis, b) Y axis, c) Z axis

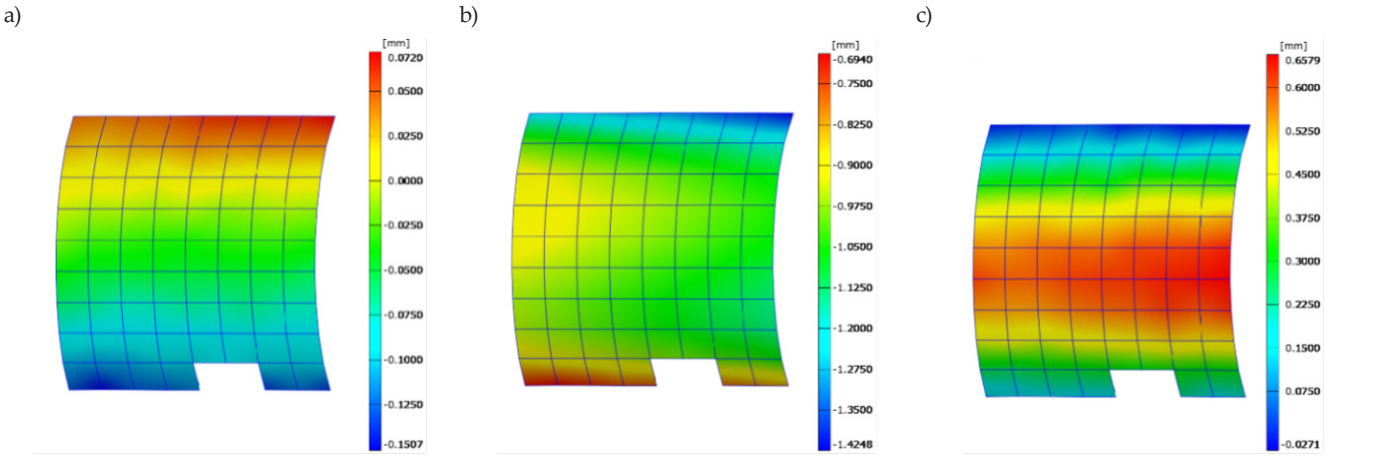

Fig. 8. Displacement distribution of P47 sample placed vertically: a) X axis, b) Y axis, c) Z axis

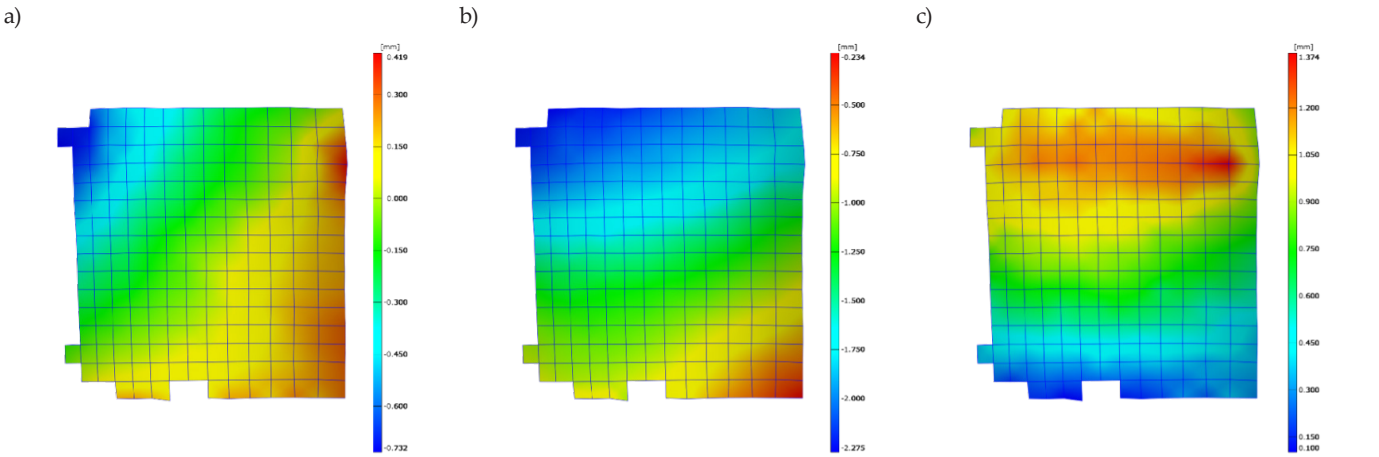

Fig. 9. Displacement distribution of P47 sample placed horizontally: a) X axis, b) Y axis, c) Z axis

and Z axes, reached values of 0.419 mm, -0.234 mm, and 1.374 mm, respectively. The displacement values in all axes are slightly larger compared to the displacements in the unfilled sample (Fig. 6). The smallest deformation area was observed for the Y axis (Fig. 6b), and the largest deformation for the Z axis (Fig. 6c). Comparing the displacement distribution maps for the unfilled sample and the sample filled with 52 wt.%, the force did not affect the slightly larger area of the filled sample. A greater force was required to fracture the sample than for the unfilled sample, suggesting a positive effect of the filler on the composite strength.

Figure 7 presents strain maps in the X, Y, and Z axes for 42 wt% filled sample positioned horizontally in the apparatus. The force used to destroy P42 composite was 0.81 kN and was significantly lower compared to both the maximum force required to destroy the sample placed

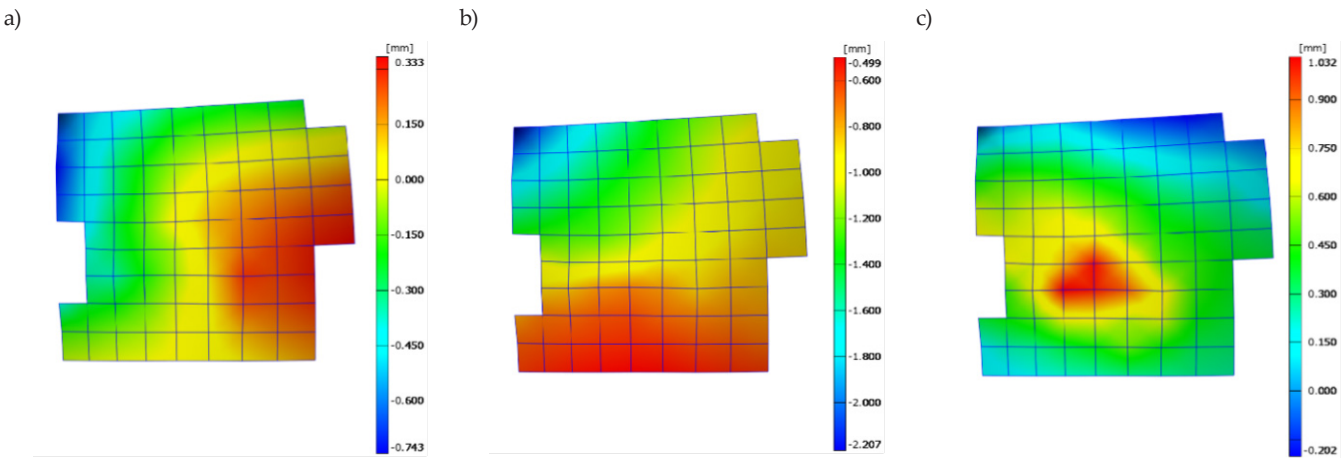

Fig. 10. Displacement distribution of P52 sample placed vertically: a) X axis, b) Y axis, c) Z axis

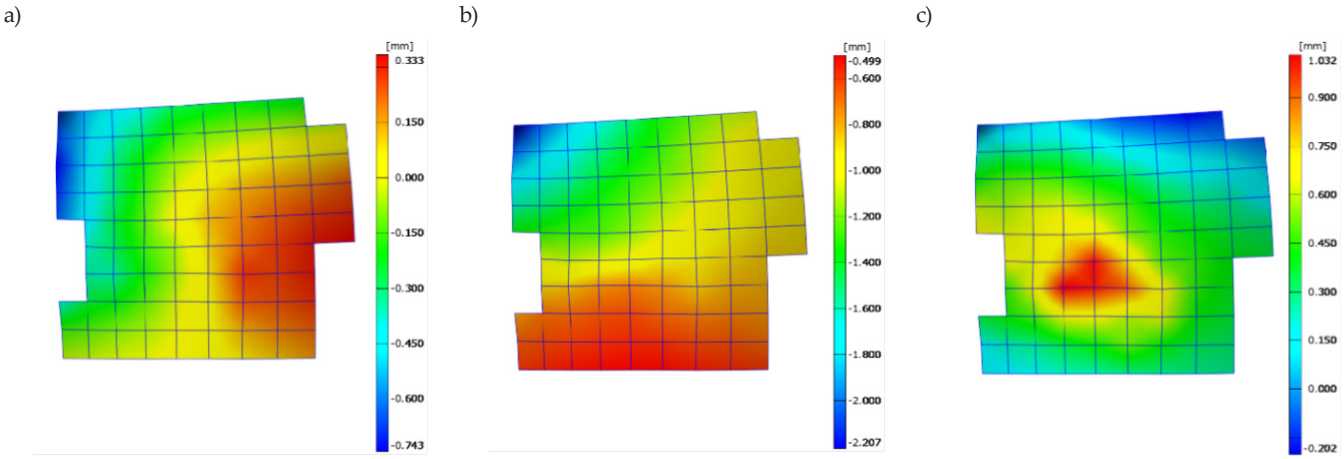

Fig. 11. Displacement distribution of P52 sample placed horizontally: a) X axis, b) Y axis, c) Z axis

vertically in the apparatus and the sample without filling. The displacements that occurred in the composite reached 0.062 mm (X axis), -0.191 (Y axis), and 0.2306 (Z axis). The largest displacement occurred along the Z axis (Fig. 7c), and the smallest along the X axis (Fig. 7a). The displacement values in all axes are significantly smaller than in the case of the unfilled sample (Fig. 7). This leads to the conclusion that filling the polymer matrix increased the composite strength.

Figure 8 shows the displacement for a vertically compressed sample containing 35 wt% $CaCO_3$ and 4 wt% each of silica, hydroxyapatite, and pearlite (total filling 47 wt%). A force was applied to the sample, the maximum value of which in the vertical orientation reached 25.67 kN. The maximum force required to destroy the sample increased compared to the force used to destroy the unfilled sample and P42 sample. The largest sample displacement occurring in the X, Y, and Z axes reached 0.251 mm, -0.272 mm, and 0.294 mm, respectively. Similarly to P42 sample, the largest displacement occurred in the Z axis (Fig. 8c), and the smallest in the X axis (Fig. 8a). The displacement in all axes is significantly smaller than in the case of the unfilled sample and P42 sample (Fig. 8). Analysis of Figures 6-8 allows us to conclude that an increase in the filling degree causes a reduction in the displacement in the samples during compression, which indicates an improvement in the mechanical strength of the composites.

Figure 9 presents strain maps in the X, Y, and Z axes for a sample positioned horizontally in the apparatus. The force applied to destroy the composite was 0.85 kN, higher than the force used to destroy P42 sample. The displacements occurring in the sample analyzed are 0.028 mm for the X axis, -0.070 mm for the Y axis, and 0.200 mm for the Z axis. The displacements are noticeably smaller compared to the unfilled sample (Fig. 4) and 42 wt% filled sample (Fig. 9). Both the increase in maximum force and the smaller displacements resulting from its action allow us to conclude that increasing the degree of filling of the polymer matrix results in an increase in the mechanical strength of the composite.

Figure 10 shows the displacements for a vertically compressed sample containing 40 wt% calcium carbonate and 4 wt% each of silica, hydroxyapatite, and pearlite (total filling 52 wt%). A force was applied to the sample, the maximum of which in the vertical position reached 20.31 kN. The maximum force required to destroy the sample was reduced compared to the force used to destroy the other samples, including the unfilled one. The largest displacement of the sample placed vertically in the

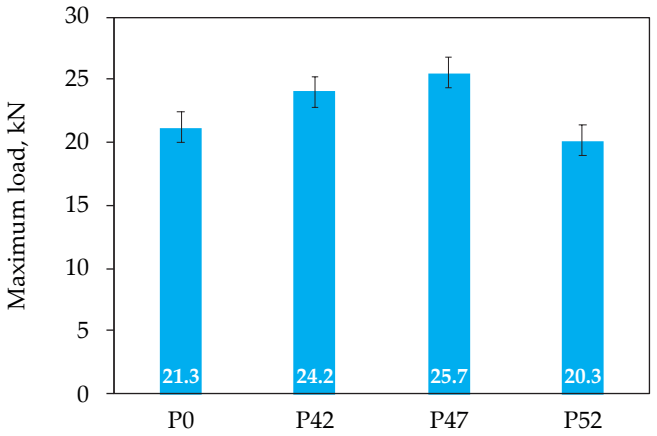

Fig. 12. Maximum load of the samples placed vertically

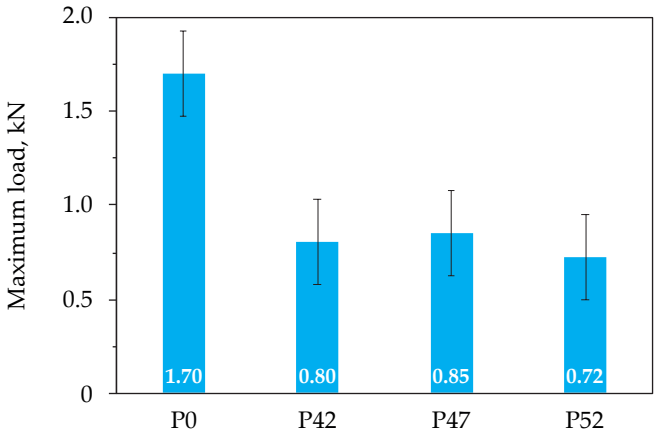

Fig. 13. Maximum load of the samples placed horizontally

apparatus, in the X, Y, and Z axes, reached -0.158 mm, -0.532 mm, and 1.330 mm, respectively. The largest displacement, albeit over a small area, occurred in the Z axis, while the largest deformation area was observed in the X axis. The maximum of the recorded displacements is significantly greater than the displacements observed in 47 wt% filled sample (Fig. 8), indicating a decrease in composite strength at such a high fill level. This leads to the conclusion that increasing the epoxy matrix fill level can only improve composite strength up to a certain saturation point. Excessive filler content can reduce matrix cohesion, resulting in reduced mechanical properties.

A force of 0.72 kN was applied to destroy sample P52 (total filling 52 wt%) placed horizontally in the apparatus. This force is approximately 28 times smaller than the force used to destroy the sample placed vertically. This indicates a lower strength of the sample compressed horizontally. Displacements reached 0.458 mm (X axis), -0.271 mm (Y axis), and 0.297 mm (Z axis). These displacements are larger compared to P47 sample (Fig. 9), indicating a lower strength of the composite. This phenomenon can be explained by the occurrence of bubbles in the prototype structure because of insufficient mold venting resulting from the large number of fillers and high viscosity of the material.

Although detailed data comparing vertical and horizontal compression tests of polymer composite cylinders with powder fillers have not been directly published, studies of related materials show that the casting and loading direction can influence mechanical properties. Specimens cast and loaded vertically often exhibit larger peak strains and better ductility, suggesting that orientation is important for mechanical properties [12, 13]. The literature emphasizes that the mechanical response of composite cylinders is sensitive both to the internal structure (e.g., filler arrangement) and to the direction of the applied force during testing [12, 13], which is precisely confirmed by the further results of our work.

The maximum load used to destroy the samples placed vertically in the apparatus (Fig. 12) increased for the samples containing 30 wt% and 35 wt% $CaCO_3$ compared to the unfilled sample, while the maximum load decreased for the sample containing 40 wt% $CaCO_3$. The highest compressive force (25.7 kN) was observed for the sample filled with 47 wt%, while the lowest (20.3 kN) was achieved for the sample with the highest fillers content (52 wt%). The obtained results allow us to conclude that increasing the filler content can improve the composite strength [14, 15], while excessive filler content weakens the polymer matrix, negatively affecting its strength. At

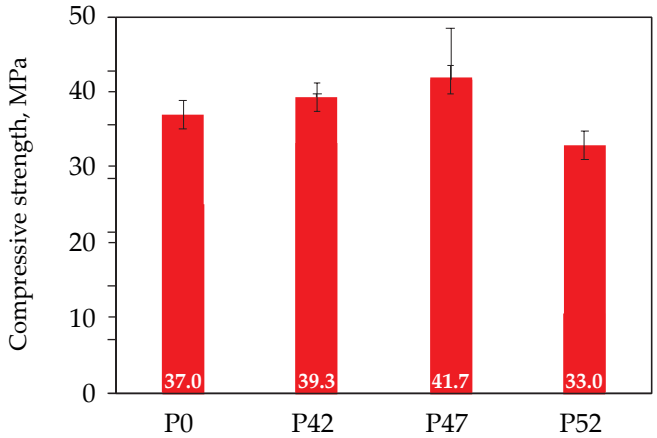

Fig. 14. Compressive strength of vertically placed samples

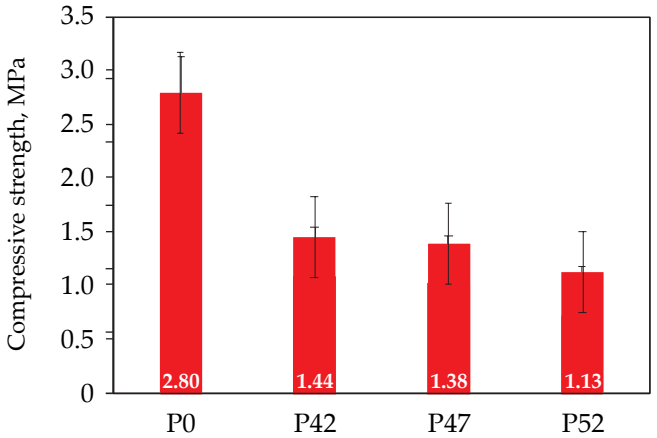

Fig. 15. Compressive strength of horizontally placed samples

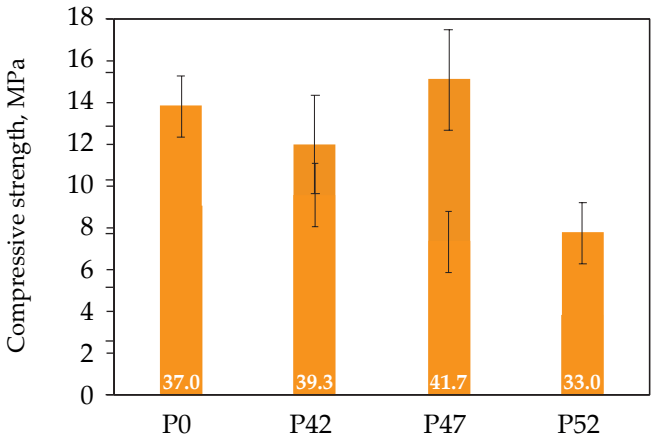

Fig. 16. Compressive strain of vertically placed samples

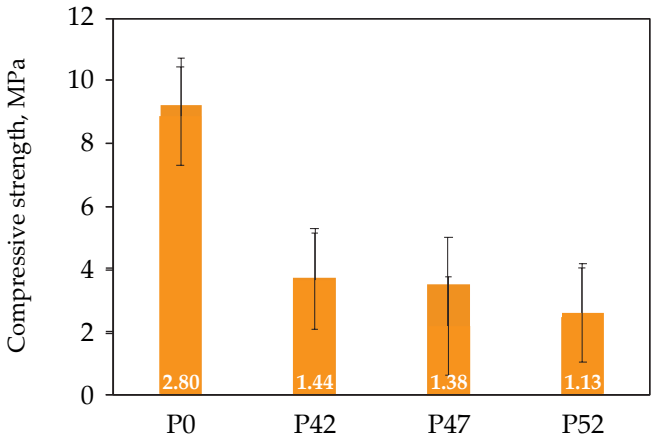

Fig. 17. Compressive strain of horizontally placed samples

low filler contents, mechanical properties can improve due to better stress transfer and filler-matrix interactions. However, as the filler content increases further, the maximum load-bearing capacity decreases due to filler agglomeration, poor dispersion, and the formation of stress concentration points [16-18].

For samples placed horizontally (Fig. 13), a decrease in the maximum load is observed for the filled samples. The addition of filler negatively affected strength, as the load required to break the filled samples was significantly lower than for the unfilled sample. The smallest decrease in the maximum load compared to the unfilled sample was observed for the sample containing 35 wt% $CaCO_3$ (P47), while the lowest load value of 0.72 kN was achieved by the sample containing 40 wt% of $CaCO_3$ (P52). Figures 12 and 13 allow us to conclude that the vertically compressed samples withstand significantly higher loads than the horizontal samples. The composites containing 35 wt% $CaCO_3$ demonstrated the highest strength.

The compressive strength changes analogously to the maximum load. Incorporating fillers increases compressive strength up to an optimal content [19-21]. For samples compressed vertically (Fig. 14), an increase in compressive strength is observed for samples containing the lowest fillers content, while for the sample with the highest fillers content, the compressive strength decreases relative to the unfilled sample. In the case of the unfilled sample, the compressive strength is about 37 MPa, while in the case of the sample containing 35 wt.% $CaCO_3$, the compressive strength reaches about 42 MPa, which indicates the high strength of the composite.

For horizontally compressed samples (Fig. 15), the compressive strength of filled samples is significantly lower than that of unfilled samples, for which the compressive strength is approximately 2.8 MPa. The highest compressive strength was demonstrated by samples containing 30 and 35 wt.% $CaCO_3$ (P42, P47), reaching a value of approximately 1.4 MPa. Furthermore, the compressive strength of horizontally compressed samples decreased with increasing fillers content. However, vertically compressed samples had significantly higher compressive strength than horizontal samples.

Although compressive strength and hardness are improved, excessive filler loading can increase brittleness [19, 20]. Compressive strain analysis showed a decrease in strain values for filled samples compared to the unfilled sample, both under vertical (Fig. 16) and horizontal (Fig. 17) compression. Vertically compressed samples achieved higher strain. Like the maximum load and compressive strength, the lowest strain under both compression conditions were observed for the sample filled with 35% $CaCO_3$ (P47), indicating the highest composite strength.

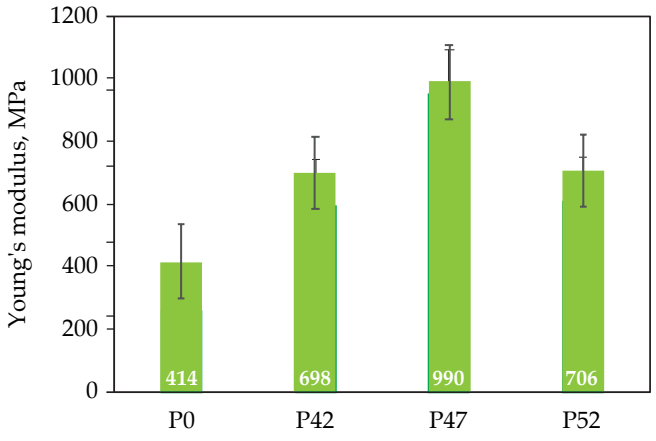

Fig. 18. Young's modulus of vertically placed samples

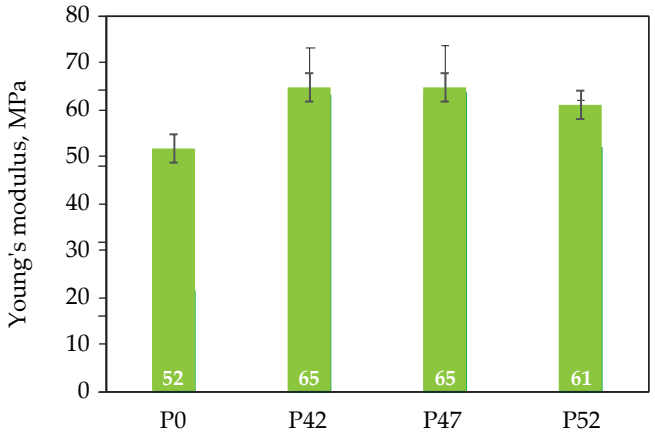

Fig. 19. Young's modulus of horizontally placed samples

a) b)

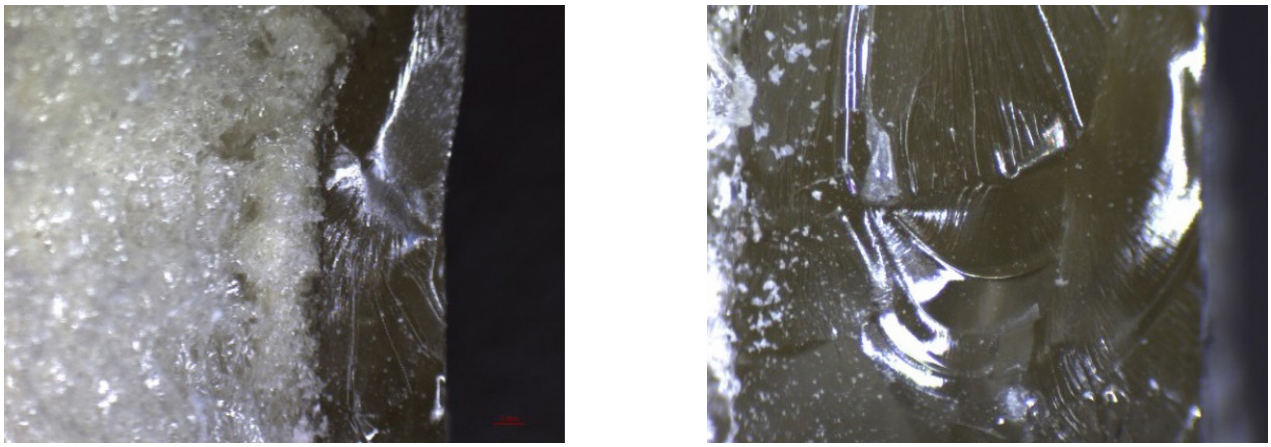

Fig. 20. Microscopic images of the cylindrical part of the prototype (sample P0): a) 2x, b) 5x magnifications

Figures 18 and 19 present Young's modulus of the tested samples. The modulus of the unfilled sample compressed vertically reaches 414 MPa, while that of the sample compressed horizontally reaches approximately 52 MPa. The highest Young's modulus was achieved for the sample containing 47 wt% fillers, reaching 990 MPa for vertical compression and 65 MPa for horizontal compression. Comparing the modulus and strain graphs, the higher the modulus value, the lower the strain [22]. The highest modulus, and therefore the lowest strain, was observed for the sample filled with 35 wt% $CaCO_3$, leading to the conclusion that this sample was characterized by the highest mechanical strength of all composites. A decrease in modulus was also observed for the samples with the highest degree of filling compared to the less filled samples.

a) b)

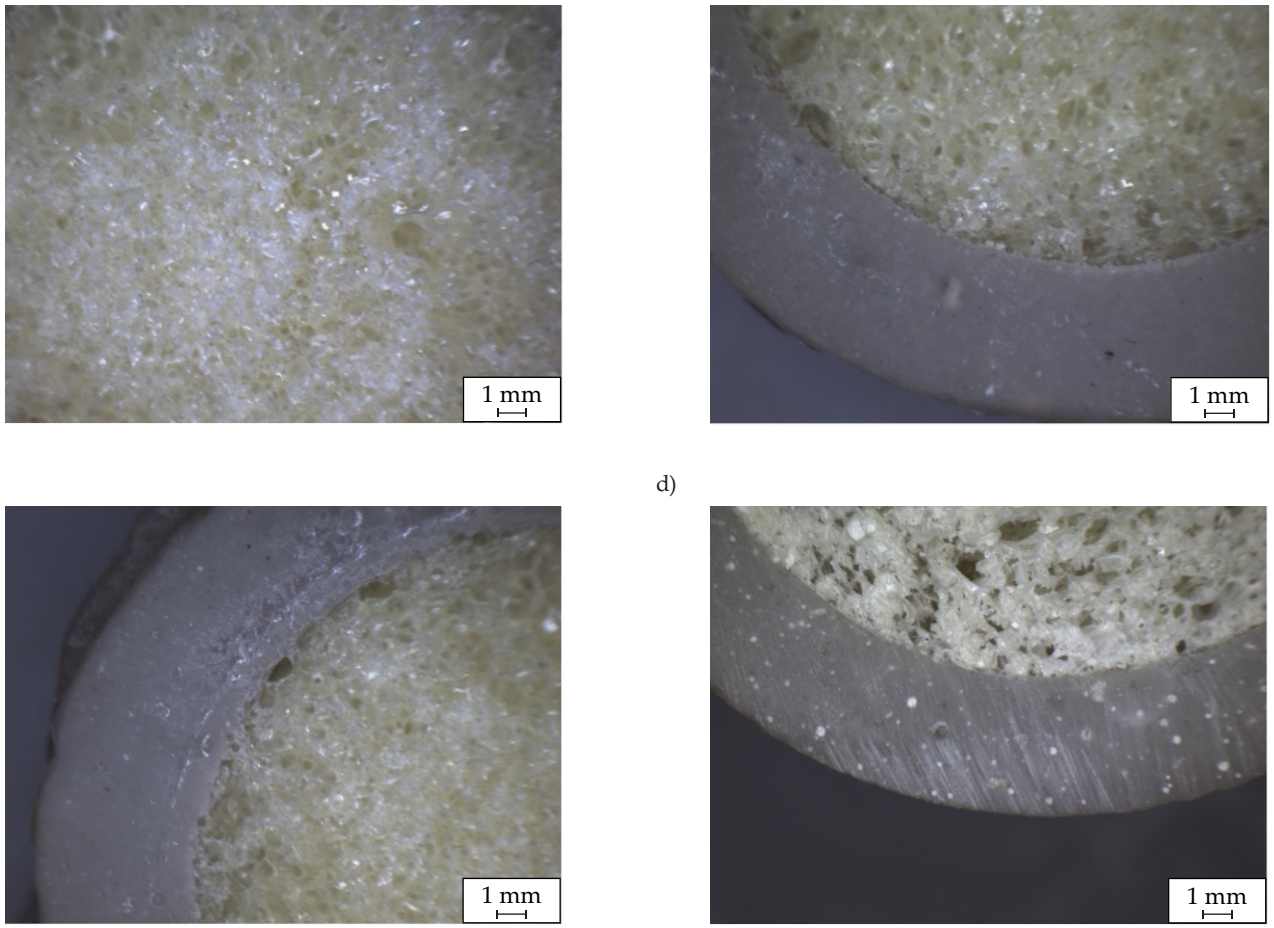

c) d)

Fig. 21. Microscopic images of the samples: a) polyurethane foam (core), b) P42, c) P47, and d) P52; 2× magnification

Summarizing the results of the static compression tests, it was found that improving the mechanical properties of composites containing calcium carbonate, hydroxyapatite, perlite, and silica is only possible up to a certain filler level [23, 24]. Excessive filler content can lead to particle agglomeration, reducing the uniformity of the filler distribution in the matrix, the formation of voids, and structural defects in the epoxy matrix, resulting in reduced matrix cohesion and, consequently, a reduction in the mechanical strength of the composites. The best mechanical properties were demonstrated by the composite containing 35 wt% calcium carbonate and 4 wt% each of hydroxyapatite, perlite, and silica, while the weakest strength was demonstrated by the composite containing 40 wt% $CaCO_3$ and the same additives. Reducing $CaCO_3$ content improves the homogeneity of the matrix, which allows for better use of the reinforcing properties of the remaining fillers.

Microscopic analysis

Figure 20 shows a microscopic image of the cylindrical part of the prototype without filling (sample P0). The crystalline and compact structure of the epoxy resin is observed. Microscopic images of the polyurethane foam used to create the core of all prototype samples are presented in Figure 21a. The open-cell structure of the foam is observed, with pore sizes ranging from 50 to 100 mm. Samples P42 (Fig. 21b), P47 (Fig. 21c), and P52 (Fig. 21d) also show porous structure, with pore sizes in the range of 0.19-0.53 mm, 0.22-0.51 mm, and 0.14-1.52 mm, respectively. The thickness of P42 and P47 composites layer is about 5.3 mm, and P52 composite 4.6 mm, which is significantly lower than for the other composites. However, sample P52 contains the largest number of pores, with the most varied sizes. Based on structural studies of the composites used to obtain cylindrical prototype shells, an increase in the number and size of pores was observed, caused by the higher filler concentration and, consequently, higher viscosity and lower air removal in the mold.

CONCLUSIONS

It was observed that increasing $CaCO_3$ content in the polymer matrix led to a significant improvement in the hardness of the composites. This effect was dependent on the filler content. Furthermore, the compressive strength of the composites improved with increasing filler content, albeit only up to a certain level. The highest compressive displacement was observed for the sample with 52 wt% fillers content, while the sample with 47 wt% fillers content showed the lowest displacement, indicating improved mechanical strength. Incorporating 42 and 47 wt% fillers into the polymer matrix resulted in higher maximum compressive load and strength, while reducing strain and increasing the compressive modulus of the vertically mounted samples. However, mechanical properties deteriorated with higher filler content (sample P52). Furthermore, the addition of fillers increased the material's porosity, and higher filler content resulted in more pores and a wider pore size distribution. Of the composites obtained, composite P42 most closely resembled the structure of natural bone. The unfilled sample showed the least similarity. These results confirm that incorporating fillers into polymer matrices improves the mechanical properties and structure of composites, making them more suitable for regenerative medicine applications.

ACKNOWLEDGMENTS
The authors would like to express their gratitude to professor Mariusz Oleksy for his laboratory and substantive support.

Authors contribution
K.B. – methodology, formal analysis, investigation, writing-original draft, visualization; D.F. – formal analysis, investigation, writing-original draft; M.O. – formal analysis, writing-original draft. All authors have read and agreed to the published version of the manuscript.

Funding
This research received no external funding.

Conflict of interest
The authors declare no conflict of interest.

REFERENCES

[1] Filip D., Bulanda K.: *Polimery* **2024**, *69(4)*, 236. htttps://doi.org/10.14314/polimery.2024.4.4
[2] Navarro M., Michiardi A., Castaño O. *et al*.: *Journal of Royal Society Interface* **2008**, *5(27)*, 1137. htttps://doi.org/10.1098/rsif.2008.0151
[3] Ratner B.D., Hoffman A.S., Schoen F.J. *et al*.: "Biomaterials Science: An Introduction to Materials in Medicine", Academic Press, Elsevier, Amsterdam 2013. htttps://doi.org/10.1016/C2009-0-02433-7
[4] Ozdil D., Aydin H.M.: *Journal of Chemical Technology and Biotechnology* **2014**, *89(12)*, 1793. htttps://doi.org/10.1002/jctb.4505
[5] Wortmann M., Frese N., Brikmann J. *et al*.: *Macromolecular Symposia* **2021**, *395(1)*, 2000242. htttps://doi.org/10.1002/masy.202000242
[6] Oleksy M., Budzik G., Kozik B. *et al*.: *Polimery* **2017**, *62(1)*, 3. htttps://doi.org/10.14314/polimery.2016.003
[7] Qulub F., Wardhani I.F.: *Indonesian Applied Physics Letters* **2023**, *4(2)*, 87. htttps://doi.org/10.20473/iapl.v4i2.48649

[8] Ferri J., Jordá J., Montanes N. *et al.*: *Journal of Thermoplastic Composite Materials* **2017**, *31(7)*, 865. htttps://doi.org/10.1177/0892705717729014
[9] Mustapha K., Ayinla R., Ottan A.S. *et al.*: *MRS Advances* **2020**, *5*, 2783. htttps://doi.org/10.1557/adv.2020.323
[10] Owais Awan M., Shakoor, A., Rehan M.S. *et al.*: *Physica B: Condensed Matter* **2021**, *606*, 412568. htttps://doi.org/10.1016/j.physb.2020.412568
[11] Masyuk A., Levytskyi V., Kechur D. *et al.*: *Chemistry, Technology and Application of Substances* **2022**, *5(5)*, 180. htttps://doi.org/10.23939/ctas2022.01.180
[12] Mansur M.A., Chin M., Wee T.H.: *Journal of Materials in Civil Engineering* **1999**, *11(1),* 21. htttps://doi.org/10.1061/(ASCE)0899-1561(1999)11:1(21)
[13] Lei C., Xie Z., Wu K. *et al.*: *Advanced Materials* **2021**, *33(49)*, 2103495. htttps://doi.org/10.1002/adma.202103495
[14] de Moura A.P., da Silva E.H., dos Santos V.S. *et al.*: *Journal of Composite Materials* **2021**, *55(21)*, 2857. htttps://doi.org/10.1177/0021998321996414
[15] Malinowski R., Fiedurek K., Rytlewski P. *et al.*: *Science of The Total Environment* **2023**, *867*, 161528. htttps://doi.org/10.1016/j.scitotenv.2023.161528
[16] Baranovska O.V., Bagliuk G.A., Buketov A.V. *et al.*: *Materials Science* **2024**, *59(5)*, 608. htttps://doi.org/10.1007/s11003-024-00817-3
[17] Manya J., Bwankwot M.T., Kambai E.D. *et al.*: *Science World Journal* **2024**, *19(2)*, 375. htttps://doi.org/10.4314/swj.v19i2.13
[18] Yildiz E., Degirmenci T., Esen M. *et al.*: *Polymer Composites* **2025**, Early view. htttps://doi.org/10.1002/pc.29706
[19] Khedri E., Karimi H.R., Mohamadi R. *et al.*: *Polymer Composites* **2024**, *45(10)*, 8694. htttps://doi.org/10.1002/pc.28369
[20] Trykoz L.V., Kamchatna S.M., Zinchenko O.S. *et al.*: *Modern Construction and Architecture* **2024**, *8*, 72. htttps://doi.org/10.31650/2786-6696-2024-8-72-79
[21] Iliyasu I., Yahaya H., Stephen M. *et al.*: *Physics Access* **2023** *3(2)*, 68. htttps://doi.org/10.47514/phyaccess.2023.3.2.011
[22] Wagner, N., McWherter, J., (2025), *Biobased Acrylate Composites with Enhanced Strength for Additive Manufacturing*, Journal of Materials Engineering and Performance, doi: htttps://doi.org/10.1007/s11665-025-10702-y
[23] Liu Z., Liu W., Ma L. *et al.*: *Polymer Composites* **2023**, *45(2)*, 1494. htttps://doi.org/10.1002/pc.27869
[24] Ali L., El Ouni M.H., Raza A. *et al.*: *Construction and Building Materials* **2021**, *308*, 125095. htttps://doi.org/10.1016/j.conbuildmat.2021.125095

Received 9 V 2025.
Accepted 24 V 2025.